Journal of Industrial Microbiology, 5 (1990) 337–354
Elsevier

SIM 245

Quantum efficiency requirements for an anaerobic photobioreactor

Andrea Maka[1] and Douglas Cork[2]

[1]*Institute of Gas Technology, and* [2]*Dept. of Biology, Illinois Institute of Technology, Chicago, IL, U.S.A.*

Received 1 August 1989
Accepted 7 August 1989

Key words: Chlorobium; Photosynthesis; Quantum efficiency; Photobioreactor; Light intensity

SUMMARY

The effect of light intensity, surface area of illuminated bioreactor, H_2S flow rate and various wavelength regions of light on oxidative sulfur metabolism by *Chlorobium* was examined. The regulation of oxidative sulfur metabolism by light intensity led to the determination of the photobioreaction quantum efficiency (PQE) for this system. This efficiency is defined as the molecules of sulfur (S°) produced per photon utilized and can be used in designing a light efficient photobioreactor. Included in our analysis of requirements for a light efficient photobioreactor is a summary of some fed-batch equations which can be used to model a productive path for the formation of sulfur during *Chlorobium*'s photosynthesis. It is suggested that the incorporation of PQE and fed-batch formulae into expressions for wavelength dependent rates of photosynthetic product formation will lead to a more accurate mathematical model for anoxygenic as well as oxygenic photosynthesis.

INTRODUCTION

A photosynthetic anaerobic bioprocess utilizing the microorganism *Chlorobium limicola forma thiosulfatophilum* (hereafter referred to as *Chlorobium*) is being investigated for the removal of acid gases (H_2S and CO_2) generated by the hydroprocessing of fossil fuels [2–5]. This process has been previously defined by the van Niel equation

$$2nH_2S + nCO_2 \xrightarrow{\text{light}} n(CH_2O) + 2nS + nH_2O \quad (1)$$

Correspondence: A. Maka, Institute of Gas Technology, 3424 South State Street, Chicago, IL 60616, U.S.A.

Chlorobium is grown in an anaerobic fed-batch photobioreactor with CO_2 as the nonlimiting carbon source, H_2S as a limiting electron source and N_2 as an inert carrier gas. The flow rate of H_2S gas into the reactor and the total light energy transmitted to the surface of the photobioreactor regulated H_2S metabolism and therefore affected the true stoichiometry of the van Niel Reaction 1 [4,5]. For example, if there is low light energy and a low H_2S flow rate, Reaction 1 shifts to Reaction 2:

$$nH_2S + 2nCO_2 + 2nH_2O \xrightarrow{\text{light}} nH_2SO_4 + 2n(CH_2O) \quad (2)$$

In addition to these two process parameters, there

are several other parameters which are believed to regulate H_2S metabolism as well as growth of the organism. These include limiting/nonlimiting CO_2, wavelength dependency, light intensity, illuminated surface area, and initial biocatalyst concentration. This paper examines quantitatively the effect of light intensity, illuminated surface area, different wavelengths of light, as well as H_2S flow rate on H_2S metabolism and growth of *Chlorobium*. These parameters are examined to determine the optimum conditions for conversion of H_2S to elemental sulfur rather than oxidation to sulfate and/or thiosulfate as well as adequate growth of the organisms.

Various wavelength regions and specific wavelengths are examined and an action spectrum, that is, the efficiency of different wavelengths of light in supporting sulfur formation of *Chlorobium* in this photobioreactor is constructed. In assessing the effect of specific wavelengths on *Chlorobium* growth and H_2S metabolism, a whole cell absorption spectrum of *Chlorobium* must be examined (Fig. 1). It indicates a strong absorption peak at 760 and 460 nm. In addition, it has been previously reported by Sybesma et al. [21] that the 840 nm wavelength is the location of the primary reaction center for *Chlorobium* photosynthesis. Hence, the specific wavelengths 760 and 840 nm are examined, as well as the wavelength regions 700 to 900 nm, 350 to 695 nm, 535 to 660 nm, 445 to 635 nm, 545 to 630 nm, and 380 to 900 nm.

By knowing that light energy controls the chemical conversion of H_2S oxidation, an approach is suggested in this paper for determining the quantum efficiency of Reaction 1, which in this system, is defined as the molecules of sulfur (S^0) produced per photon utilized.

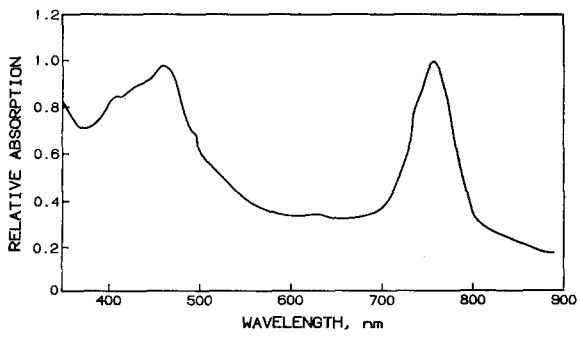

Fig. 1. Absorption spectrum of *Chlorobium*.

MATERIALS AND METHODS

Microorganism

Chlorobium limicola forma thiosulfatophilum ATCC 17092 was used in this study. The defined growth medium is referred to as 1X, which is a mineral salts medium. [16] For all trials, the microorganism was prepared and 'activated' as described previously. [5]

Chlorobium chlorophyll concentration was determined by measuring bacteriochlorophyll spectrophotometrically at 670 nm. [20] The specific growth rate (μ) of *Chlorobium* was calculated from the chlorophyll concentration by the following equation:

$$\mu = \frac{k}{X} \tag{3}$$

in which k is the slope of a plot of chlorophyll concentration versus time (see below for calculation) and X is the chlorophyll concentration. In the range of light intensities examined in the well defined bioreactor utilized in this study, there was a direct correlation between *Chlorobium* chlorophyll/ml, the mg of cells/ml, and the number of cells/ml [16].

The following are sample calculations for the determination of specific growth rate. Light intensity values were those examined in the white light region (380 to 900 nm). Plots of chlorophyll concentration (mg/l) versus time (hours) at several light intensity values are presented. From the plots (Fig. 2), k (the slope) is determined and defined as:

$$k = \frac{X_{17} - X_0}{t_{17} - t_0} \tag{4}$$

in which X_{17} is the final chlorophyll concentration of the cells at A_{670} and X_0 is the initial chlorophyll concentration of the cells at A_{670}. Time is in hours, t_{17} is the final hour (17th hour), and t_0 is the initial hour. The slope (k) varies with light intensity, and

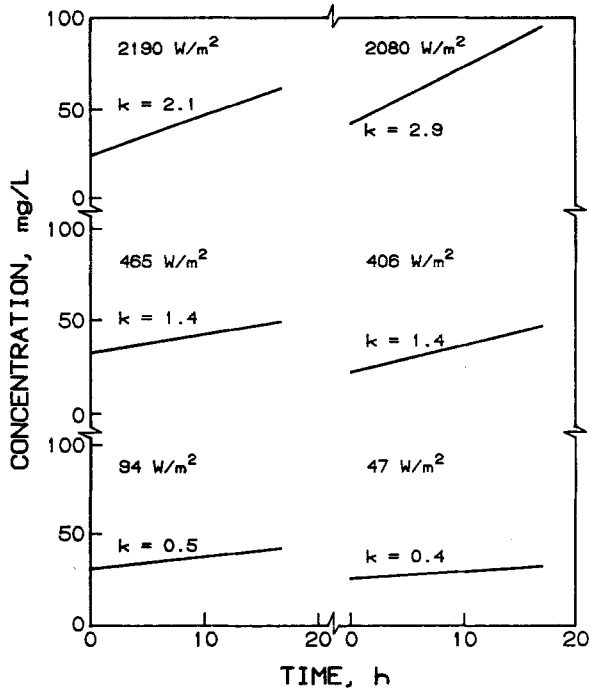

Fig. 2. Sample plots to determine k values. Light intensity (W/m^2) values selected from white light region (Table 1).

the specific growth rate decreases as the cell concentration increases. For example, at a light intensity of 465 W/m^2:

$$\mu_0 = \frac{k}{X_0} = \frac{1.4 \text{ mg/l} \cdot \text{h}}{29 \text{ mg/l}} = 0.05 \text{ h}^{-1} \quad (5)$$

$$\mu_{17} = \frac{k}{X_{17}} = \frac{1.4 \text{ mg/l} \cdot \text{h}}{52 \text{ mg/l}} = 0.03 \text{ h}^{-1} \quad (6)$$

and at a light intensity of 47 W/m^2:

$$\mu_0 = \frac{k}{X_0} = \frac{0.4 \text{ mg/l} \cdot \text{h}}{26 \text{ mg/l}} = 0.02 \text{ h}^{-1} \quad (7)$$

$$\mu_{17} = \frac{k}{X_{17}} = \frac{0.4 \text{ mg/l} \cdot \text{h}}{33 \text{ mg/l}} = 0.01 \text{ h}^{-1} \quad (8)$$

The absorption spectrum of *Chlorobium* whole cells (Fig. 1) was determined by placing the cells in the path of the light source of a Zeiss Spectrophotometer and scanning from 350 to 900 nm. The cells were diluted 1:4 in a 10% sucrose solution. The reference cuvette contained 2 ml of a 10% sucrose solution.

Fed-batch reactor designs

This reactor was characterized in previous studies [15,16]. Gas-fed continuously stirred reactors were used in all experiments. Gas cylinders of CO_2 (anaerobic grade $\geq$99.99% purity, $\leq$10 ppm oxygen), H_2S ($\geq$99.9% purity), and N_2 ($\geq$99.9% purity), $\leq$10 ppm oxygen) were used as the source of all substrates. The gas blending and flow were strictly maintained by Tylan mass flow gas controllers. Other details of the process (pH, temperature control, etc.) have been previously described. [5,16]

Light sources were placed outside the reactor chambers at defined positions to ensure light saturation. The positions and number of light sources varied depending upon experimental conditions. The light source for activation of the organism, was a 250-W tungsten halogen lamp placed 22 cm from the surface of the reactor. The entire cylindrical reactor was exposed to the light source. The position and number of light sources for the light analysis experiments are described below.

Due to high initial bacterial concentrations (ca. 5.0 $\times$ 10^8 cell/ml), there was limited light availability for the photosynthetic reaction inside of the reactor. Photons were absorbed at the surface layer normal to the light source as determined by a radiometer. The fed-batch process was examined quantitatively, with respect to this light limitation, using cylindrical reactors with light sources normal to a defined surface area. Initially, this surface area was found to be 144 cm^2. Therefore, the entire reactor was covered with aluminium foil except the 144 cm^2 area normal to the light sources. The light source for one reactor was a 250-W tungsten halogen lamp placed 22 cm from the surface of the reactor. The second reactor was illuminated by three light sources: 100-W and 150-W incandescent phototungsten bulbs and a 150-W reflector bulb. These were placed 24 cm from the reactor surface.

For studies that examined the effect of infrared light on *Chlorobium* sulfur metabolism and growth, the exposed 144 cm^2 surface area described previously was covered with blocking filters. Specifically

pairs No. 874 and No. 823 or No. 866 and No. 817 were placed over the defined area. These filters allowed light of only longer wavelengths than 700 nm to enter the reactor.

For specific surface area/light intensity experiments, the 144 cm^2 surface area was reduced to either 32, 48, or 64 cm^2. In these instances, the entire reactor was covered with aluminium foil except for various 4 cm × 4 cm windows which were exposed normally to each light source. The light sources were four 300-W light bulbs. Two light sources were placed 17 cm from the center of the reactor. The other two were placed 21 cm from the center of the reactor. These light sources were attached to variacs to manipulate light intensities.

Photobioreactor theory

The photobioreactor was the basic reactor described above with an exposed surface area of 64 cm^2 (four windows of dimensions 4 cm × 4 cm). The entire reactor was covered with aluminium foil except for the 64 cm^2 area exposed to the light

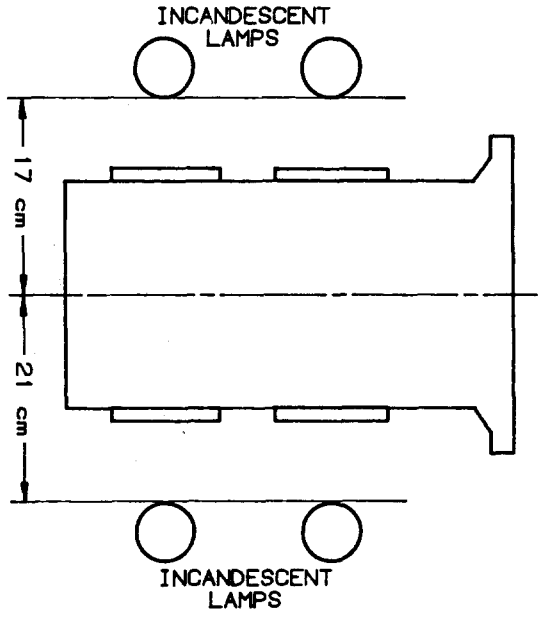

Fig. 3. Photobioreactor — four filters of the desired wavelengths are placed on the reactor. The light sources were four 300-W incandescent light bulbs. Two light sources are placed 17 cm normal to the reactor surface containing two filters. Two light sources are placed 21 cm normal to the reactor surface containing the other two filters.

sources. Due to the limited size of the reactor, two filters were taped on each of two opposite sides of the reactor, as shown in Fig. 3. The filters were flat pieces of glass, whereas the reactor surface was curved. For the filters to lie flat on the curved surface of the reactor, a layer of padding 1 cm thick was placed between the reactor surface and filter. The padding was placed along the edges of the 5 cm × 5 cm filters.

Four 760 nm or 840 nm interference filters of dimensions 5 cm × 5 cm and standard thickness 2.5 mm were utilized in studies that examined the effect of these wavelengths on sulfur metabolism and growth.

Blocking filter combinations No. 823 and No. 874 or No. 817 and No. 866 were utilized in studies that examined the effect of greater than 700 nm light on sulfur metabolism and growth. These were flexible plastic sheets of dimensions 8 inches × 10 inches and were simply taped on the reactor.

Colored glass filters were utilized in the remaining wavelength experiment. These glass filters are 5 cm × 5 cm of standard thickness 2.5 mm, except CM500 with a standard thickness of 1 mm. The following filters were employed: G533 (selected for 445 to 635 nm) and CM500 (selected for 350 to 695 nm). To select for the narrow wavelength bands, 535 to 660 nm and 545 to 630 nm, the combination color glass filter CM500 and blocking filter No. 817 and color glass filter G533 and No. 817 blocking filter were used, respectively. To prevent water from entering into the color glass filters and into the interference filters, the edges of the filters were sealed with paraffin.

The transmission spectra for all glass filters (GM500 and G533), interference filters (760 and 840 nm), blocking filters, and combinations of glass and blocking filters were determined by placing the filters in the path of the light source of a Zeiss Spectrophotometer and scanning from 350 to 900 nm.

The total light energy transmitted through the surface of the reactor was detected by a radiometer (Yellow Springs Instruments Co., Yellow Springs, Ohio, Model 65A), which was placed at either 12 different positions (for the 144 cm^2 surface area) or

9 different positions (for the 32, 48, and 64 cm^2 surface area) along the inside frontal surface of the defined area. The 12 values for the 144 cm^2 were integrated by using the formula:

$$W = \int_0^9 \int_0^{16} I((y,h)\, dy,dh \tag{9}$$

Where W is the light energy in watts per square centimeter, I is the detected light power in watts, y is the width in centimeters, and h is the height in centimeters. The nine values were integrated by using the formula:

$$W = \int_0^4 \int_0^4 I(y,h)\, dy,dh \tag{10}$$

$$E = (6.63 \times 10^{-34}\ J \cdot s) \times \frac{3 \times 10^{10}\ cm/s)}{(8.00 \times 10^{-5}\ cm)} = 2.49 \times 10^{-19}\ J \tag{11}$$

Number of photons absorbed:

$$\frac{8.57 \times 10^4\ J\ (\text{total energy entering reactor})}{2.49 \times 10^{-19}\ J\ (\text{energy of a photon})} = 3.44 \times 10^{23} \tag{12}$$

The number of molecules of sulfur formed from mmoles of sulfur are determined from a typical Avogadro calculation:

$$\frac{9.7 \times 10^{-3}\ mol \times 6.02 \times 10^{23}\ molecules}{mol} = 5.84 \times 10^{21}\ molecules \tag{13}$$

Therefore, the quantum efficiency was:

$$\frac{5.84 \times 10^{21}\ (\text{molecules of sulfur formed})}{3.44 \times 10^{23}\ (\text{photons absorbed})} = 0.017 = 1.7\% \tag{14}$$

The quantum requirement was:

$$\frac{1}{0.017} = 59 \tag{15}$$

Experimental conditions and analytical procedures

Gas flow rates were set at the beginning and

The nine values for each 4 cm × 4 cm window were integrated separately and then added cumulatively to give total watts for the 32, 48, or 64 cm^2 surface area.

For determination of quantum efficiencies and quantum requirements, the average wavelength of each wavelength region was selected. The wavelength regions and total energy values selected were those at which maximal conversion of H_2S to sulfur was observed, that is, 85% to 97% sulfur production.

A typical quantum efficiency calculation is presented below. For example, the average wavelength in the region 700 to 900 nm is 800 nm. The total power entering the reactor was 1.4 W (1.4 J/s). This was a 17-h (6.12×10^4 s) study and 9.7 mmol of sulfur were produced. The total energy entering the reactor, that is, 8.5×10^4 J was determined by multiplying the total power entering the reactor, that is, 1.4 J/s times the length of the study, that is 6.12×10^4 s.

The energy of a photon defined by $E = hv$ at 800 nm is:

monitored and controlled by Tylan Control Valves. All trials were 17 hours. Sample aliquots (10 ml) were withdrawn for analytical determinations. All techniques for analysis of elemental sulfur, sulfate, thiosulfate, and soluble sulfide were as previously described. [19,16,22]

RESULTS

Effect of light intensity on chlorobium sulfur metabolism and growth

Tables 1 and 2 present the effect of light intensity on metabolism and growth in the presence of white

Table 1

Effect of reactor light intensity on *Chlorobium* sulfur metabolism and growth at a 64 cm^2 surface area and a constant H_2S molar flow rate of 1 mmol/l-h in the presence of white light (380 to 900 nm)[a]

Light intensity		Oxidized sulfur compounds, %[b]				Growth variables[c]	
W/64 cm^2	W/m^{2d}	S^0	$S_2O_3^{2-}$	SO_4^{2-}	S^{2-}	$\mu_0(h^{-1})$	$(h^{-1})\mu_{17}$
4.9	766	10	24	65	0[e]	0.15	0.04
2.6	406	60	40	0	0	0.07	0.03
1.0	156	70	0	1	30	0.01	0.01
0.6	94	72	0	1	27	0.02	0.01
0.3	47	54	0	4	4	0.02	0.01

a Unfiltered light from incandescent phototungsten bulb (380 to 900 nm).

b Calculated on a molar basis: Average of three trials; 100% is total sulfur equivalents.

c $\mu_0 = \frac{k}{X_0}$, $\mu_{17} = \frac{k}{X_1}$ where k = slope of growth curve and X_0 and X_{17} are mg chlorophyll/l at times 0 and 17 hours of growth.

d Light energy value expressed in international units.

e For all 0%, this signifies that the value is below the sensitivity of the assay.

Table 2

Effect of reactor light intensity on *Chlorobium* sulfur metabolism and growth at a 64 cm^2 surface area and a constant H_2S molar flow rate of 1 mmol/l-h in the presence of infrared light (700 to 900 nm)

Light intensity		Oxidized sulfur compounds, %[a]				Growth variables[b]	
W/64 cm^2	W/m^{2c}	S^0	$S_2O_3^{2-}$	SO_4^{2-}	S^{2-}	$\mu_0(h^{-1})$	$(h^{-1})\mu_{17}$
4.0	625	24	29	46	0	0.11	0.04
3.5	547	56	7	37	0	0.10	0.04
1.4	219	97	3	0	0	0.05	0.03
0.3	47	28	4	0	67	0.02	0.01

a Calculated on a molar basis: Average of three trials; 100% is total sulfur equivalents assayed after 17 hours.

b $\mu_0 = \frac{k}{X_0}$, $\mu_{17} = \frac{k}{X_{17}}$ where k = slope of growth curve and X_0 and X_{17} are mg chlorophyll/l at times 0 and 17 hours of growth.

c Light intensity expressed in international units.

light (380 to 900 nm), and infrared light (700 to 900 nm), respectively. The H_2S molar flow rate was kept constant at 1 mmol/l · h. The surface area illuminated was 64 cm^2. In the presence of white light, reducing the light intensity from 766 to 406 W/m^2 resulted in the increased production of elemental sulfur and thiosulfate and the decrease in sulfate formation (Table 1). At light intensities of 156 W/m^2 or less there is H_2S accumulation and inhibition of growth as evidenced by a reduction in the specific growth rate (see Materials and Methods for calculations of specific growth rate). Adequate growth (a specific growth rate difference of 0.03 or greater) occurred at the higher intensities.

Table 2 presents the effects of various infrared light intensity levels. A maximal light intensity of 625 W/m^2 was detected on the surface of the reactor by our integral method of analysis (see Materials and Methods). Blocking filters that were selected for the 700 to 900 nm light were placed over the 64 cm^2 surface area and reduced the transmitted light intensity. As the light intensity levels decreased from 625 to 219 W/m^2, the production of elemental sulfur increased to greater than 90% with thiosulfate and sulfate production almost ceasing. At a light intensity of 47 W/m^2, H_2S oxidation does not occur. Hence, there is H_2S accumulation and inhibition of growth. Adequate growth occurred at the higher intensities.

Effect of light intensity on specific growth rate

Adequate growth at the higher light intensities and reduction of the specific growth rate at the lower light intensities at the same nonlimiting substrate concentration suggested there was a direct relationship between specific growth rate and light intensity. Previous studies have shown that the growth of *Chlorobium* is linear and the rate of growth (dX/dt) is some constant value greater than zero [9,15]. The growth is described by:

$$\frac{dX}{dt} = \mu X \tag{16}$$

Where μ is the specific growth rate, and X is the chlorophyll concentration (mg/l). The product (μX) is some constant value greater than zero. As the chlorophyll concentration (X) increases, the specific growth rate (μ) decreases. As the chlorophyll concentration (X) increases, the dense cell suspension will prevent the entering light from being absorbed. Therefore, the specific growth rate (μ) is dependent upon light intensity (LI) and can be described by:

$$\frac{k}{X} = \mu \tag{17}$$

$$\therefore\ k \text{ is proportional to LI} \tag{18}$$

Where k is obtained from the slope of a plot of chlorophyll concentration versus time (see Materials and Methods for calculations) and X is chlorophyll concentration. As the light intensity (LI) entering the reactor increases, the specific growth rate (μ) increases. Fig. 4 presents a plot of k versus LI. The values for k increase as the light intensity increases. As k increases, the specific growth rate (μ) increases. The above determinations are based on experimental data in which there was no breakthrough of H_2S and the H_2S concentration in the medium was constant.

Effect of surface area on Chlorobium sulfur metabolism and growth

Tables 3 and 4 present the effect of surface area on *Chlorobium* sulfur metabolism and growth in the presence of white light and infrared light, respectively. The use of blocking filters to select for the 700

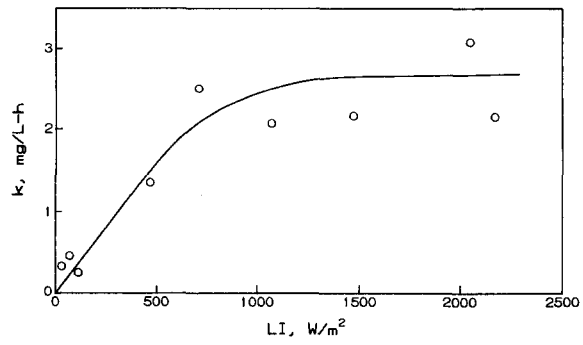

Fig. 4. Plot of k versus LI. LI are the light intensity values examined in the white light region (380 to 900 nm).

Table 3

Effect of reactor surface area[a] on *Chlorobium* sulfur metabolism and growth at a constant H_2S molar flow rate of 1 mmol/l-h and constant power in the presence of white light (380 to 900 nm)

Surface area,[b] cm^2	Power, Watts[e]	Light intensity, W/m^{2f}	Oxidized sulfur compounds, %[c]				Growth variables[d]	
			S^0	$S_2O_3^{2-}$	SO_4^{2-}	S^{2-}	$\mu_0(h^{-1})$	$(h^{-1})\mu_{17}$
144	6.7	465	10	10	80	0	0.08	0.04
64	6.9	1080	19	17	65	0	0.05	0.03
48	6.6	1380	20	15	65	0	0.10	0.03
32	6.8	2130	85	13	0	0	0.06	0.03

[a] The total surface area, i.e. length by width of exposed reactor.
[b] A description of the dimensions for each of these surface areas is described in the Materials and Methods section.
[c] Calculated on a molar basis: Average of three trials: 100% is total sulfur equivalents assayed after 17 hours.
[d] $\mu_0 = \frac{k}{X_0}$, $\mu_{17} = \frac{k}{X_{17}}$ where k = slope of growth curve and X_0 and X_{17} are mg chlorophyll/l at times 0 and 17 hours of growth.
[e] Constant absolute value of power irrespective of the surface area.
[f] Light intensity value expressed in international units.

Table 4

Effect of reactor surface area[a] on *Chlorobium* sulfur metabolism and growth at a constant H_2S molar flow rate of 1 mmol/l-h and constant power in the presence of infrared light (700 to 900 nm)

Surface area[b] cm^2	Power watts[e]	Light intensity, W/m^{2f}	Oxidized sulfur compounds, %[c]				Growth variables[d]	
			S^0	$S_2O_3^{2-}$	SO_4^{2-}	S^{2-}	$\mu_0(h^{-1})$	$(h^{-1})\mu_{17}$
144	1.5	104	98	2	0	0	0.05	0.03
64	1.5	219	97	3	0	0	0.05	0.03
48	1.4	313	97	13	0	0	0.05	0.03
32	1.6	500	87	11	0	0	0.05	0.03

[a] The total surface area, i.e. length by width of exposed reactor.
[b] A description of the dimensions for each of these surface areas is described in the Materials and Methods section.
[c] Light intensity values expressed in international units.
[d] Calculated on a molar basis: Average of three trials; 100% is total sulfur equivalents assayed after 17 hours.
[e] $\mu_0 = \frac{k}{X_0}$, $\mu_{17} = \frac{k}{X_{17}}$ where k = slope of growth curve and X_0 and X_{17} are mg chlorophyll/l at times 0 and 17 hours of growth.
[f] Constant absolute value of power irrespective of the surface area.

to 900 nm wavelength region limited the amount of power transmitted through the reactor surface, hence the same amount of power employed for white light could not be obtained. The values selected were based on the maximum amount of power detected at the reactor surface at a defined surface area of 32 cm^2. With an increase in surface area, the power of the light sources was reduced to make the power, that is, watts, equivalent to the watts at 32 cm^2. Four surface areas (144, 64, 48, and 32 cm^2) were examined. The effect of these surface areas in the presence of white light with approximately 6.7 watts of power transmitted to these areas is presented in Table 3. At a 32 cm^2 area, elemental sulfur accumu-

lated. Increasing the surface area to 48 and 64 cm^2, sulfur production decreased, thiosulfate remained relatively the same, and sulfate increased significantly. Table 4 presents the effect of surface area in the presence of infrared light. Elemental sulfur was the major product at all surface areas. The production of sulfur decreased slightly at the reduced surface area of 32 cm^2.

Effect of H_2S flow rate on Chlorobium sulfur metabolism and growth

The effect of H_2S flow rates on H_2S metabolism and growth at various defined surface areas (144, 64, and 32 cm^2) and light intensities are presented in Tables 5 and 6. Two flow rate values (1 and 2 mmol/l-h) were examined. Table 5 presents the effect of H_2S flow rate in the presence of white light. Under conditions of high light intensity, 2080 and 2190 W/m^2, sulfur formation increased and sulfate decreased as the H_2S flow rate increased from 1 to 2 mmol/l-h. A reduction in power from 30 to 2 Watts transmitted to the bioreactor surface (144 cm^2) resulted in elemental sulfur as the major product at 1 mmol/l-h and sulfide accumulation at 2 mmol/l-h.

Table 6 presents the effect of H_2S flow rate in the presence of infrared light. In the presence of higher light intensities, that is, 625 W/m^2 and approximately 350 W/m^2, at the higher flow rate, elemental sulfur was the major product. Decreasing the light intensity to 63 W/m^2, resulted in elemental sulfur being the major product at the reduced flow rate.

Effect of wavelengths on Chlorobium sulfur metabolism and growth

Table 7 examines the effect of various wavelength regions on *Chlorobium* growth and H_2S metabolism at a defined surface area of 64 cm^2, an H_2S flow rate of 1 mmol/l-h and a relatively constant light intensity of 1 W/64 cm^2. The organisms were able to grow in the visible and/or infrared regions of light. In the narrow band region, 535 to 660 nm and 545 to 630 nm, absorption of light by the organism was minimal. Therefore, neither growth nor production of the various sulfur species was expected (though these two light regions are close, the region 545 to 630 nm was further selected to obtain as narrow a light region as possible where absorption is minimal). However, at these wavelength regions, the data confirmed active growth and sulfur metabolism. Throughout all of the wavelength regions examined, elemental sulfur was the predominant product with exclusive production of sulfur taking place in the infrared wavelength region. There was no oxidation and therefore accumulation of H_2S

Table 5

Effect of H_2S molar flow rate on *Chlorobium* sulfur metabolism and growth at constant surface area and power in the presence of white light (380 to 900 nm)

H_2S Molar flow rate, mmol/l-h	Power, Watts	Surface area, cm^2	Light intensity, W/m^2 [c]	Oxidized sulfur compds. %[a]				Growth variables[b]	
				S^0	$S_2O_3^{2-}$	SO_4^{2-}	S^{2-}	$\mu_0(h^{-1})$	$(h^{-1})\mu_{17}$
2	2	144	139	90	0	0	10	0.05	0.03
1	2	144	139	97	3	0	0	0.05	0.03
2	30	144	2080	85	7	4	0	0.07	0.03
1	30	144	2080	16	7	78	0	0.07	0.03
2	7	32	2190	85	13	0	0	0.05	0.02
1	7	32	2190	55	10	35	0	0.06	0.03

[a] Calculated on a molar basis: Average of three trials, 100% is total sulfur equivalents assayed after 17 hours.

[b] $\mu_0 = \frac{k}{X_0}$, $\mu_{17} = \frac{k}{X_{17}}$ where k = slope of growth curve and X_0 and X_{17} are mg chlorophyll/l at times 0 and 17 hours of growth.

[c] Light intensity expressed is international units.

Table 6

Effect of H_2S molar flow rate on *Chlorobium* sulfur metabolism and growth at constant surface area and power in the presence of infrared light (700 to 900 nm)

H_2S Molar flow rate, mmol/l-h	Power, Watts	Surface area, cm^2	Light intensity, Watts/m^2 [c]	Oxidized sulfur compds. %[a]				Growth variables[b]	
				S^0	$S_2O_3^{2-}$	SO_4^{2-}	S^{2-}	$\mu_0(h^{-1})$	$(h^{-1})\mu_{17}$
2	0.9	144	63	73	2	0	28	0.02	0.01
1	0.9	144	63	98	2	0	0	0.05	0.03
2	5.0	144	347	98	0	4	0	0.03	0.01
1	5.1	144	354	31	13	56	0	0.04	0.01
2	4.0	64	625	87	13	0	0	0.09	0.04
1	4.0	64	625	24	29	46	0	0.10	0.04

[a] Calculated on a molar basis: Average of three rials, 100% is total sulfur equivalents assayed after 17 hours.

[b] $\mu_0 = \frac{k}{X_0}$, $\mu_{17} = \frac{k}{X_{17}}$ where k = slope of growth curve and X_0 and X_{17} are mg chlorophyll/l at times 0 and 17 hours of growth.

[c] Light intensity expressed in international units.

Table 7

Effect of wavelengths on *Chlorobium* sulfur metabolism and growth at a constant surface area, and H_2S molar flow rate[a]

Wavelengths, nm	Light intensity W/64 cm^2	Total photons absorbed, $\times 10^{22}$	Oxidized sulfur compounds, %[b]				Growth variables[c]	
			S^0	$S_2O_3^{2-}$	SO_4^{2-}	S^{2-}	$\mu_0(h^{-1})$	$(h^{-1})\mu_{17}$
White light								
380–900	1.0	20	70	0	1	30	0.01	0.01
700–900	1.4	34	97	3	0	0	0.05	0.03
350–695	1.3	21	85	18	0	0	0.04	0.02
535–660	0.9	17	85	14	0	0	0.08	0.03
445–635	1.4	23	62	37	0	0	0.09	0.04
545–630	0.5[d]	9.1	91	10	0	0	0.05	0.03
760	0.3[e]	6.9	34	0	0	66	0.01	0.01
840	0.3[e]	7.5	33	0	0	67	0.01	0.01

[a] 1 mmol/l-h.

[b] Calculated on a molar basis: Average of three trials, 100% is the total sulfur equivalents assayed after 17 hours.

[c] $\mu_0 = \frac{k}{X_0}$, $\mu_{17} = \frac{k}{X_{17}}$ where K = slope of growth curve and X_0 and X_{17} are mg chlorophyll/l at times 0 and 17 hours of growth.

[d] 0.5 is the maximal amount of light intensity.

[e] 0.3 is the maximal amount of light intensity. Description of filters and their arrangement on reactor described in the Materials and Methods section.

and inhibition of growth in the single wavelength regions 760 and 840 nm because of the low light intensities transmitted to the reactor. Also, in the presence of white light, there was inhibition of growth due to sulfide accumulation. Thiosulfate formation was observed in all of the wavelength regions less than 700 nm as was an enhancement of growth. A specific growth rate difference of 0.05 was observed in the visible regions of 535 to 660 nm and 445 to 635 nm. Analyses of these phenomena

(thiosulfate formation in the presence of visible light and growth and production of the various sulfur species in the narrow band region 545 to 630 nm and 535 to 660 nm) will be presented in the discussion section.

Table 7 also presents the values for the energy of a photon of light at the selected wavelength regions. There is an inverse relationship between the energy of a photon of light at a selected wavelength and the wavelength of light. An analysis of this observation of H_2S oxidation will also be presented in the discussion section.

DISCUSSION

Light and electron dependent regulation of H_2S oxidation

Light intensity, illuminated surface area, and H_2S flow rate regulate H_2S metabolism (Tables 1 through 6). Figs. 5 through 10 summarize the results obtained in this paper. Figs. 5 and 6 present the effect of increasing H_2S flow rate on oxidative sulfur metabolism. Figs. 7 and 8 present the effect of increasing light energy (power in the presence of icreased and decreased H_2S flow-rate) on oxidative sulfur metabolism. Optimal sulfur production is observed at decreased flow rate in the presence of low energy input (Figs 6 and 7). In the presence of increased H_2S flow rate, optimal sulfur production is observed at relatively low energy input and remains relatively constant as the energy is increased (Fig. 8). Conditions are suboptimal when either sulfate production is favored or there is sulfide breakthrough. The production of sulfate is favored as the energy input increases in the presence of reduced H_2S flow rate (Fig. 7). Sulfide breakthrough occurs in the presence of increased H_2S flow rate and low energy input (Figs. 6 and 8). Also evident in Figs. 5 to 10 is the formation of low levels of thiosulfate. The regulation of sulfur metaboism and growth in *Chlorobium* involves control of all enzymes involved in the 64 electron oxidation of hydrogen sulfide to sulfate.

$$8H_2S \xrightarrow{\text{Reaction 1}} S^8 \xrightarrow{\text{Reaction 2}} 8SO_4^{2-} \quad (19)$$

16 electrons orthorhombic sulfur 48 electrons

This is a 64-electron oxidation as shown in Equation 19 because the elemental sulfur produced is deposited as orthorhombic sulfur, which, of course, has a valence of zero on each of eight sulfur atoms. Therefore, the oxidation of H_2S to sulfur involves a 16 electron oxidation with complete oxidation via H_2S to sulfate producing 64 electrons. These reducing electrons ultimately flow to CO_2 for carbon assimilation. Light intensity, H_2S molar flow rate and illuminated surface area will control the 'rate' of electron flow. The 16 electron oxidation of H_2S to sulfur provides sufficient reducing power for CO_2 fixation, if light and H_2S are in sufficient and continuous supply. This can be observed under conditions of low light intensity and reduced H_2S flow rate conditions. Under these conditions, photons may be described as a limiting substrate for *Chlorobium* resulting in insufficient energy to drive the oxidation reaction to optimal completion, that is, sulfate production (Reaction 2). Increasing the amount of light favors production of thiosulfate and sulfate. Under conditions of high light intensity and reduced H_2S flow rate (Tables 2 and 6), the high light input stimulates CO_2 fixation. Therefore, the organisms further oxidize the sulfur to sulfate to generate the 48 electrons required for the additional CO_2 fixation. A schematic diagram demonstrating this cyclic coupling effect has been previously published. [5]

Regulation of sulfur metabolism was not wavelength dependent (Table 7). The organisms grew and oxidized H_2S in any selected wavelength region (except at 760 and 840 nm where the low light intensity transmitted to the reactor surface was inadequate for H_2S metabolism and growth). However, the rate at which H_2S oxidation proceeded was wavelength dependent. The energy of a photon of light at each wavelength is different. In the infrared region of light (700 to 900 nm), the average wavelength (800 nm) has an energy of 2.49×10^{-19} Joules (for calculation see the Materials and Methods section on calculating quantum efficiency). In the visible region of light (350 to 645 nm), the average wavelength (523 nm) has an energy of 3.8×10^{-19} Joules. Therefore, the energy of a photon of a particular wavelength of light in the visible region is greater than the energy of a photon of a particular

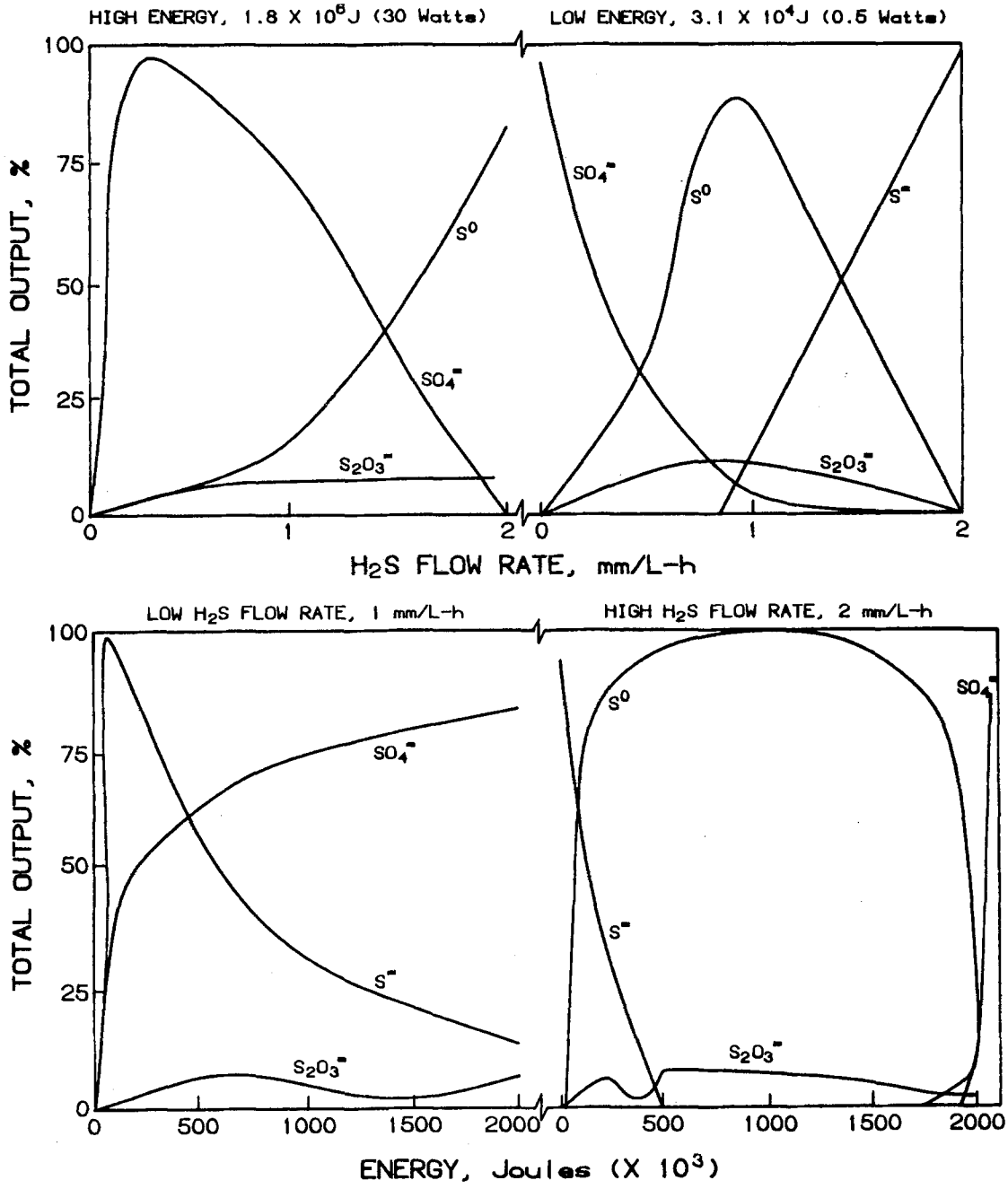

Figs. 5 and 6. Effect of increasing H_2S flow rate on oxidative sulfur metabolism in the presence of high and low light energy. Total output is based on the presence of oxidized sulfur products after 17 hours of growth. For conversion of Watts to Joules, 1 W = 1 J/s.

wavelength in the infrared region. The data suggest that *the greater the inherent energy of a photon, the faster the rate of H_2S oxidation.* The oxidized sulfur products increase slightly when the organisms are grown in the visible regions of light (except 545 to 620 nm light region). The maximal amount of light intensity transmitted to the reactor surface in the 545 to 630 nm region was 0.5 W/64 cm^2. This reduced light intensity may have favored sulfur formation. If the light intensity could have been increased to

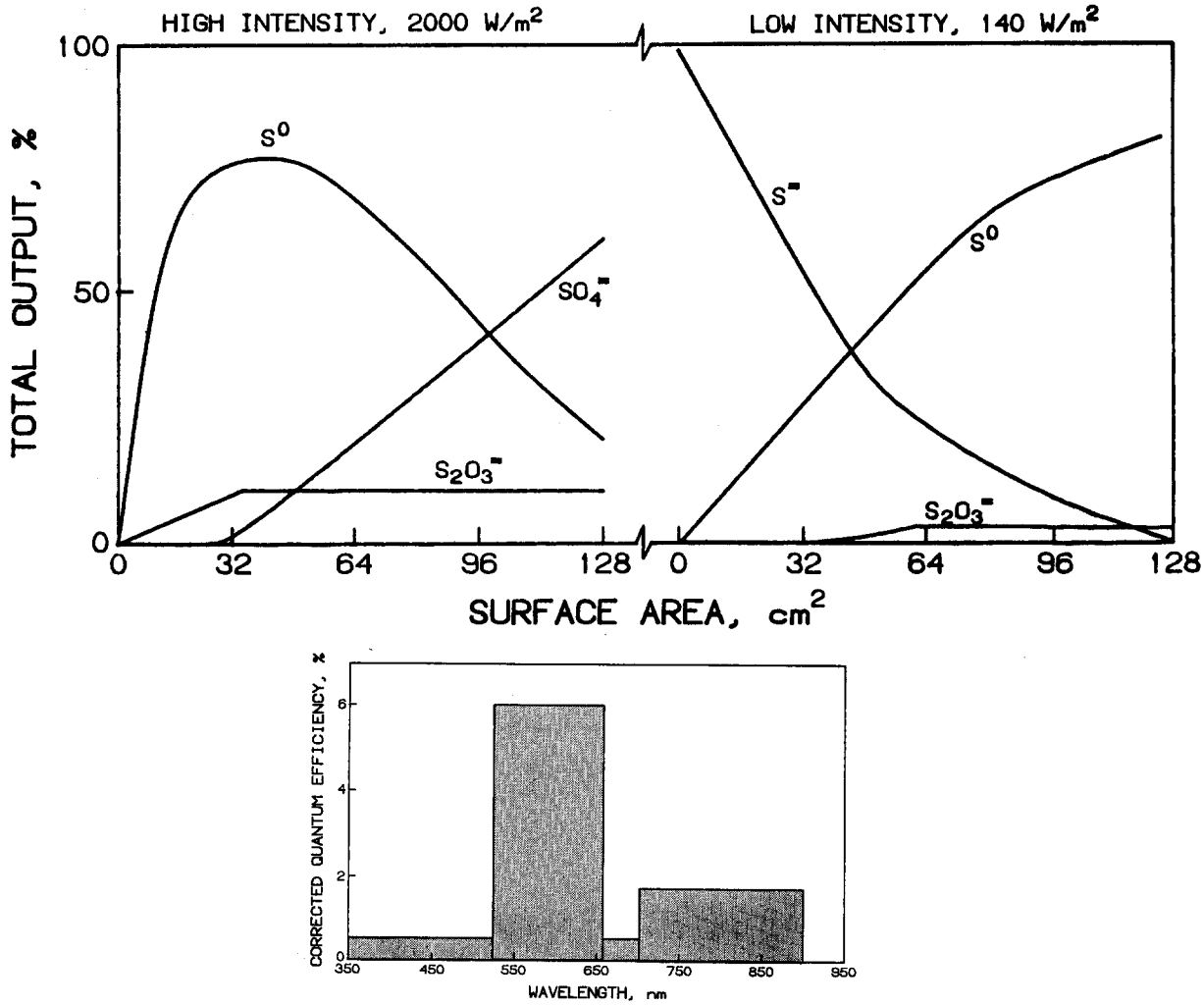

Figs. 7 and 8. Effect of increasing light energy on oxidative sulfur metabolism in the presence of low and high H_2S flow rate. Total output is based on the percent of oxidized sulfur products after 17 hours of growth. For conversion of Watts to Joules, 1 W = 1 J/s.

values equivalent to those obtained in the other visible regions, increased production of the oxidized sulfur products would probably have been observed. For example, in the infrared region, 97% of the H_2S was converted to sulfur, whereas in the visible region (445 to 635 nm), 62% of the H_2S was converted to sulfur and 37% to thiosulfate (Table 7).

Quantum efficiency

The regulation of H_2S metabolism by light established with these data led to the determination of the photosynthetic quantum efficiency for this system. The quantum efficiency is defined as the molecules of sulfur formed per number of photons of light utilized. Also, relevant is the quantum requirement of this system, which is the number of photons absorbed per sulfur molecule formed or simply the reciprocal of quantum efficiency. Table 8 presents the quantum efficiency and quantum requirement of this reaction at several wavelength regions (for calculations of quantum efficiencies and quantum requirements see Materials and Methods). Fig. 1 is the action spectrum of *Chlorobium* presented as a bar graph. The graph illustrates the efficiency of different wavelengths of visible and infrared light in supporting sulfur formation. The action spectrum

does not coincide with the absorption spectrum of *Chlorobium* (Fig. 1) between 350 and 660 nm. *Chlorobium* has an absorption maxima in the visible region at 460 nm, however, the quantum efficiency between 350 and 535 nm is low. Maximum efficiency is observed between 535 to 660 nm where absorption by the organism is minimal. In the region between 660 to 900 nm, the action spectrum does coincide with the absorption spectrum. In the region between 660 to 700 nm, where absorption by the organism is minimal, the efficiency is low. In the infrared region where *Chlorobium* has an adsorption maxima at 760 nm, the quantum efficiency increases.

The growth of *Chlorobium* and concomitant metabolism of H_2S in 535 to 630 nm and 545 to 630 nm light is unexpected because absorption of these wavelengths by the organism is minimal. The organism contains the light absorbing bacteriochlorophyll pigments as well as the accessory carotenoid pigments. The bacterial pigments do not absorb light in the region 535 to 660 nm and the carotenoids absorb minimally in this region [17]. However, *Chlorobium* does contain bacteriochlorophyll a (20% of the total chlorophyll content). Bacteriochlorophyll a does have an absorption maximum at 590 nm [17]. It may be that Bchl a is absorbing the 590 nm light when the cells are grown in the presence of 535 to 660 nm light and then internally transfer the energy to a higher wavelength of 840 nm, the photoreaction center of *Chlorobium*. Alternatively, it may be that the cytochromes in this region, particularly the flavocytochrome C-553, absorb light and are photooxidized with the energy being transferred to P_{840}. *Chlorobium* does contain cytochrome C-551, flavocytochrome C-553, and cytochrome C-555 [12–14]. The later model can be used to explain the higher rates of sulfide oxidation previously shown because the presumed sulfide oxidase, C-553, is involved.

The low quantum efficiency obtained for our reaction suggests that large amounts of light energy are required to drive the conversion of H_2S to sulfur. However, conversion of H_2S to sulfur is an exothermic dark reaction [16]. In our determination of quantum efficiency, we have assumed that elemental sulfur is the only product formed at the expense of light energy. However, because we are working with whole cells, there are other photoproducts such as ATP and NADPH required for biosynthesis [1]. Therefore, in working with whole cells, we are

Table 8

Quantum efficiencies and quantum requirements

Wavelength, nm	Light energy	% mmol of S^0 produced	Quantum efficiency, (Q.E.)[a], % (φ)	Quantum requirements, ($1/\varphi$)
700–900	1.4	97	1.7	59
350–695	1.3	85	2.5	40
535–660	0.5	89	5.8	17
545–660	0.5	91	6.0	17
350–535	–	–	0.5[b]	200
660–700	–	–	0.5[b]	200

[a] Q.E. is defined as the ratio of the molecules of sulfur produced to the number of photons absorbed at the average wavelength of a defined wavelength region.

[b] Values are corrected quantum efficiency calculated as follows:

$$\frac{(\lambda_{695\,nm} - \lambda_{350\,nm})\,(Q.E._{350\,nm/695\,nm}) - (\lambda_{660\,nm} - \lambda_{535\,nm})\,(Q.E._{535\,nm/660\,nm})}{(\lambda_{535\,nm} - \lambda_{350\,nm}) + (\lambda_{700\,nm} - \lambda_{660\,nm})}$$

Description of equation in Appendix A.

actually considering all the photoproducts of biosynthesis, not just sulfur, though we are attempting to define quantum efficiency with respect to the single product sulfur. To determine accurately the photons required for H_2S conversion to sulfur, this reaction must be uncoupled from the other biosynthetic processes of the cell. In other words, the low quantum efficiency of the H_2S to S^0 reaction confirms that this is a dark reaction, but is coupled to a light driven oxidation pathway [5].

Many determinations of the photosynthetic quantum efficiency of green plants and bacteria have been attempted, though no definite value has emerged [6,7,18,25]. A variety of experimental approaches have been used by investigators to determine photosynthetic quantum efficiency, which is generally defined as the molecules of O_2 evolved per photon of light utilized [18,25]. At present, there is no coherent method to determine bioreactor quantum efficiency for the good of biotechnological productivity.

We feel our assessment of quantum efficiency for this system is more accurate than that made by other investigators for green plant photosynthetic quantum efficiency for several reasons. In green plant photosynthesis, errors arise in determination of O_2 evolution due to its consumption during respiration concurrent with its evolution during photosynthesis. In *Chlorobium* under our semi-batch reactor growth conditions in which H_2S, as the accessory hydrogen donor for photosynthesis, is continuously supplied to the organism during photosynthesis, sulfur is deposited extracellularly and not utilized by the cells. We can control the fed-batch concentration of H_2S, that is, the donor in our photosynthetic system. On the other hand, H_2O, the donor in green plant photosynthesis, is always 55.55 M. The donor concentration (H_2S) is less than the acceptor concentration (CO_2) in our system. Due to our control of the H_2S concentration in the fed-batch design, we are able to see how light affects H_2S conversion. This is not the case with substrate H_2O in green plant photosynthesis.

The determination of quantum efficiency is essential when working with a photobioreactor because it can be used to design an efficient photobioreactor. The photosynthetic quantum efficiency can be used as a efficiency factor for a photobioreactor. The efficiency factor would be a unique characteristic of the reactor and would show the relationship between light intensity and the rate of a photosynthetically driven reaction. It would be expressed in terms of quantum efficiency and determined in a similar manner as quantum efficiency.

Chlorobium fed-batch analysis

This efficiency factor can then be used to define more accurately other models of photosynthesis. For example, we have seen that *Chlorobium* has a specific growth (μ) which is a function of both a growth limiting substrate (S) and the intensity of light (LI) in the reactor. That is:

$$\mu = \mu_1(S)\mu_2(\mathrm{LI}) \tag{20}$$

The substrate hydrogen sulfide is inhibitory and therefore μ is described by:

$$\mu_1(S) = \frac{\mu_{\max} S}{K_S + S + K_I S^2} \tag{21}$$

The variable μ_2 can also be expressed as:

$$\mu_2(\mathrm{LI}) = K_{\mathrm{LI}}(\mathrm{LI}) \tag{22}$$

Chlorobium is grown in a fed-batch fermentor where the substrate is added slowly enough so that its concentration in the broth is kept low in order to prevent inhibition. Further, the substrate is added to the fermentor in the form of a gas which is highly soluble in the broth. This substrate is quickly dissolved in the liquid phase and so it is the rate of the microbial reaction which limits substrate utilization. Also, the volume of the fermentor liquid remains essentially constant during the course of the fermentation, that is, the dissolution of the gaseous substrate has almost no effect on the reactor volume.

When the flow rate, F, and composition, S_I, of the gas stream into the reactor are held constant, it is found that the concentration of substrate in the broth is maintained at a constant low value. Therefore, we can delineate the fed-batch material balance

equation which applies to this process and show that they lead to the conclusion:

$$-r_S = \frac{FS_I}{V} \tag{23}$$

and

$$r_X = Y_{X/S}\frac{F}{V}S_I \tag{24}$$

See Appendix B for derivation of r_S and r_X. Knowing that $dX/dt = r_X$ and that this is a constant $= Y_{X/S}F/V\,S_I$, then

$$Y_{X/S}\frac{F}{V}S_I = \mu_1(S)\,\mu_2(\mathrm{LI})\,X = \mu_1(S)\,K_{LI}(\mathrm{LI})X \tag{25}$$

Since $\mu_1(S)$ = a constant, therefore:

$$(\mathrm{LI})X = \frac{Y_{X/S}\dfrac{F}{V}S_I}{\mu_1(S)\,K_{LI}} = \text{a constant} = K \tag{26}$$

$$(\mathrm{LI}) = \frac{K}{X} \tag{27}$$

Light utilization analysis

Included among the equations utilized in the development of models for photosynthesis are specific light utilization expressions. These light utilization expressions are a function of the specific absorbance of the light that is utilized by the microorganism at specific wavelengths (Equations 28 and 29). When extrapolated, these expressions can be used to quantitate the specific rate of light absorption by the organisms (Equations 30 and 31) [10,11]. See Appendix A for an explanation of variables.

$$u \cdot \nabla I(\chi,\lambda,u) = -[\Sigma_a(\lambda) + \Sigma_s(\lambda)]I(\chi,\lambda,u) + \iint_{4\pi}\Sigma_s(\lambda)I(\chi,\lambda,u')\rho\lambda(u',u)d\omega' \tag{28}$$

$$I_a = \int_{v}\int_{0}^{\infty}\iint_{4\pi}\Sigma_a(\lambda)I(\chi,\lambda,u)d\omega d\lambda dv \tag{29}$$

$$\xi = \frac{I_a}{X \cdot V} \times 10^3 \tag{30}$$

$$\xi = \frac{1}{V}\int_{v}\int_{0}^{\infty}\iint_{4\pi}\sigma_a(\lambda)\,\delta(x,\lambda,u)d\omega d\lambda dv \tag{31}$$

According to Aiba's analysis, ξ can be used in a general mathematical formulation for photosynthetic growth by *Rhodopseudomonas spheroides S* [10,11]:

$$\mu = \mu_{max}\xi\, f(S) \tag{32}$$

$$= \frac{\xi - b}{a}\cdot\frac{S}{K_S + S} \tag{33}$$

The incorporation of the fed batch expressions (Equations 20 through 27) and the quantum efficiency of the working photobioreactor into the specific light utilization expressions (Equations 28 through 33) may lead to a more accurate and specific photosynthetic model for *Chlorobium*. This model can be used to predict an optimization policy for *Chlorobium* in a well defined fed-batch reactor, and is an ongoing research goal in our labs.

ACKNOWLEDGEMENTS

This research was supported in part by the Institute of Gas Technology's in-house research and development program, Project No. 20275 and in part by the Tennessee Valley Authority (TVA) and Advanced Bio-Kinetics, Int., Muscle Shoals, Alabama, 35662. We also thank Dr. William Weigand for his contributions to the fed-batch analysis.

APPENDIX A

Definitions for fed-batch equations

μ = specific growth rate
μ_1 = specific growth rate as a function of substrate concentration
μ_2 = specific growth rate as a function of light intensity
S = the growth limiting substrate in the medium
S_I = composition of the inflow gas in the fed-batch reactor
μ_{max} = maximal specific growth rate
K_S = Monod substrate constant
K = light intensity constant
K_I = inhibitory substrate constant
LI, I = light intensity
r_S = substrate reaction rate
r_X = cell concentration rate
F = flow rate
V = volume
$Y_{X/S}$ = cell yield
X = cell concentration

Definitions for corrected quantum efficiency equation

$\lambda_{695\,nm} - \lambda_{350\,nm}$ = the difference of the wavelength region 695 − 350
$Q.E._{.350\,nm\ -\ 695\,nm}$ = the quantum efficiency for the wavelength region 350–695
$\lambda_{535\,nm} - \lambda_{350\,nm}$ = The difference of the wavelength region 535 − 350
$\lambda_{700\,nm} - \lambda_{660\,nm}$ = The difference of the wavelength region 700 − 660
$\lambda_{660\,nm} - \lambda_{535\,nm}$ = The difference of the wavelength region 660 − 535
$Q.E._{.535\,nm\ -\ 660\,nm}$ = The quantum efficiency for the wavelength region 535–600

Definitions of Aiba's light efficient growth expressions

u = unit vector
I = local light intensity
λ = wavelength
χ = position vector
$\Sigma(\lambda)$ = sectional area per unit volume as a function of λ either absorbed (a) or scattered (s) wavelengths (λ)
$\rho\lambda(u,u)$ = phase function for $u' \rightarrow u$
a = empirical constant
b = empirical constant
I_a = light energy absorbed
V,v = volume
ξ = specific light absorption rate
ω = solid angle, steradian

APPENDIX B

Derivation of r_X and r_S for fed-batch reaction

F, S, and S_I are constant

$$FS_I + Vr_S = \frac{d(VS)}{dt} = \frac{V dS}{dt}$$

$$\frac{dS}{dt} = \frac{F}{V} S_I + r_S$$

Since S is constant, $\frac{dS}{dt} = 0$

$$0 = \frac{F}{V} S_I + r_S$$

$$-r_S = \frac{F}{V} S_I$$

Since V is constant, $\frac{dV}{dt} = 0$

$$\frac{d(VX)}{dt} = Vr_X$$

$$\frac{V\,dX}{dt} = Vr_X$$

$$\frac{dX}{dt} = r_X$$

$$\frac{r_X}{r_S} = -Y_{X/S} = \text{constant}$$

$$r_X = -Y_{X/S} r_S$$

$$r_X = Y_{X/S} \frac{F}{V} S_I$$

Since $\frac{dX}{dt} = r_X = Y_{X/S} \frac{F}{V} S_I$, where F, V, S_I and $Y_{X/S}$ are all constant a plot of X versus t will have a constant slope equal to $r_X = Y_{X/S} \frac{F}{V} S_I$

REFERENCES

1 Chain, R.K. and D.I. Arnon, 1977. Quantum Efficiency of Photosynthetic Energy Conversion. Proc. Natl. Acad. Sci. U.S.A., 74: 3377–3381.

2 Cork, D.J. 1981. Bioconversion of Coal Acid Gas to Biomass and Chemicals. Paper presented at the Midwest Energy Conference on Liquid Fuels From Coal and Biomass. Modwest Universities Energy Consortium, Ohio State University, Columbus, Ohio, Oct. 5 and 6.

3 Cork, D.J., R. Garunas and A. Sajjad. 1983. *Chlorobium limicola forma thiosulfatophilum* Biocatalyst in the Production of Sulfur and Organic Carbon From a Gas Stream Containing H_2S and CO_2. Appl. Env. Microbiol. 45: 913–918.

4 Cork, D.J. and S. Ma. 1982. Acid-Gas Bioconversion Favors Sulfur Production. Biotechnical Bioeng. Symp. 12: 285.

5 Cork, D.J., J. Mathers, A. Maka and A. Srnak. 1985. Control of Oxidative Sulfur Metabolism in *Chlorobium limicola forma thiosulfatophilum*. Appl. Environ. Microbiol. 49: 269–272.

6 Emerson, R. 1958. Some Factors Influencing the Long-Wave Light of Photosynthesis. Ann. Rev. Plant Physiol. 9: 1–24.

7 Emerson, R. and C.M. Lewis. 1943. The Dependence of the Quantum Yield of *Chlorella* Photosynthesis on Wavelengths of Light. Am. J. Botany 30: 165–174.

8 Jensen, S.L. 1978. Chemistry of Carotenoid Pigments. In: The Photosynthetic Bacteria. (Clayton, R.K. and W.R. Sistron, eds.), Plenum Press, New York.

9 Kakidas, L.B. 1978. Bioconversion of Hydrogen Sulfide and Carbon Dioxide to Starch by *Chlorobium limicola forma thiosulfatophilum*. M.S. Thesis, Illinois Institute of Technology, Chicago, IL.

10 Koizumi, J. and S. Aiba. 1981. Optimal Design of Bio-Photoreactor: Parallel-Plate Reactor. Biotechnical Bioeng. 23: 657–662.

11 Koizumi, J. and S. Aiba. 1980. Significance of the Estimation Light-Absorption Rate in the Analysis of Growth of *Rhodopseudomonas spheroides*. Eur. J. Appl. Microbiol. Biotechnol. 10: 113–123.

12 Kusai, A. and T. Yamanaka. 1973a. Cytochrome *c* (553 *Chlorobium thiosulfatophilum*) is a Sulfide-Cytochrome *c* Reductase. FEBS Lett. 34: 235.

13 Kusai, A. and T. Yamanaka. 1973b. A Novel Function of Cytochrome *c* (555, *Chlorobium thiosulfatophilum*) in Oxidation of Thiosulfate. Biochem. Biophys. Res. Commun. 1: 107–112.

14 Kusai, A. and T. Yamanaka. 1973c. The Oxidation Mechanism of Thiosulfate and Sulfide in *Chlorobium thiuosulfatophilum*: Roles of Cytochrome *c*-551 and Cytochrome *c*-553. Biochim. Biophys. Acta. 325: 304–314.

15 Ma, S. 1982. The Control of Sulfur Metabolism in *Chlorobium limicola forma thiosulfatophilum*. M.S. Thesis, Illinois Institute of Technology, Chicago, IL.

16 Maka, A.D. 1986. Control of Oxidative Sulfur Metabolism in *Chlorobium*. Ph.D. Thesis, Illinois Institute of Technology, Chicago, IL.

17 Pfenning, N. 1978. General Physiology and Ecology of Photosynthetic Bacteria. In: The Photosynthetic Bacteria. (R.K. Clayton and W.R. Sistrom, eds.), pp. 3–18, New York: Plenum Press.

18 Pirt, J.S., Y. Lee, A. Richmond and N.W. Pirt. 1980. The Photosynthetic Efficiency of *Chlorella* Biomass Growth With reference to Solar Energy Utilization. J. Chem. Tech. Biotechnol. 30: 25–34.

19 Sorbo, B. 1957. A Colorimetric Method for the Determination of Thiosulfate. Biochim. Biophys. Acta. 23: 412–416.

20 Stanier, R.Y. and J.H.C. Smith. 1960. The Chlorophylls of Green Sulfur Bacteria. Biochim. Biophys. Acta. 41: 478–484.

21 Sybesma, C. and W. J. Vredenberg. 1964. Kinetics of Light-Induced Cytochrome Oxidation and P_{840} Bleaching in Green Photosynthetic Bacteria Under Various Conditions. Biochim. Biophys. Acta. 88: 205–207.

22 Tabatabai, M.A. 1974. Determination of Sulfate in Water Samples. Sulfur Inst. J. 10: 11–13.

23 Truper, H.G. and H.G. Schlegel. 1964. Sulfur Metabolism in *Thiorhodaceae* I. Quantitative Measurements on Growing Cells of *Chromatium okenii*. J. Microbiol. Serol., Antonie van Leeuwenhoek, 30: 225–235.

24 Van Gemerden, H. 1968. Growth Measurements of *Chromatium* Cultures. Arch. Mikrobiol. 64: 103–110.

25 Warburg, O. and E. Negelein. 1923. Uber den Einfluss der Wellenlange auf den Energiemusatz Bei der Kohlen-Saure-assimilation. Z. Phys. Chem. 106: 191–20.